International Research Journal of Basic and Clinical Studies Vol. 8(4) pp. 1-14, August, 2023
Available online http://www.interesjournals.org/IRJBCS

Review Article

Graphitic Carbon Nitride Quantum Dots (g-C3N4): Fundamentals and Applications

Lyano H Madkour*

Prof. Loutfy H. Madkour: Professor of Physical chemistry, Nanoscience and Nanotechnology Chemistry Department, Faculty of Science, Tanta University, 31527, Tanta, Egypt

*Corresponding Author's E-mail: lya_madkour@yahoo.com, lya.madkour@gmail.com;

(Egypt)

Received: 01-Aug-2023, Manuscript No. irjbcs-23-107710; **Editor assigned:** 04-Aug-2023, PreQC No. irjbcs-23-107710 (PQ); **Reviewed:** 18-Aug-2023, QC No. irjbcs-23-107710; **Revised:** 25-Aug-2023, Manuscript No. irjbcs-23-107710 (R); **Published:** 31-Aug-2023, DOI: 10.14303/irjbcs.2023.48

Abstract

As a novel C and N based two-dimensional material, graphitic carbon nitride quantum dots (g-C3N4) QDs is regarded as a new generation of photocatalyst and has been widely used in the field of environmental photocatalysis. In recent years, graphitic carbon nitride has become one of the very exciting sustainable materials, due to its unusual properties and promising applications as a heterogeneous catalyst in water splitting and organic contaminant degradation. A variety of modifications have been reported for this nanostructured material with the use of carbonaceous materials to enhance its potential applications. Carbon nitrides (C3N4) are renowned organic semiconductors with a band gap of 2.7 eV, which are connected via tri-s-triazine-based forms. Graphitic carbon nitride (g-C3N4) is considered as an attractive, efficient and newly generated promising visible light–driven photocatalyst ascribable material owing to its distinct properties such as metal free, suitable band gap, chemical inertness and high physicochemical stability. Nevertheless, the photocatalytic activity of pure g-C3N4 was limited by the fast recombination rate of photoinduced electron–hole pairs, poor photoexcited charge separation, limited range of visible light absorption and relatively low specific surface area. Enhanced photocatalytic activity is achievable by the construction of homojunction nanocomposites to reduce the undesired recombination of photogenerated charge carriers. The formed g-C3N4 isotype heterojunction photocatalyst manifested significant improvement photocatalytic hydrogen production than the single and pure g-C3N4 sample. This significant enhanced photocatalytic performance is mainly ascribed to inhibited recombination, enriched active site and enlarged specific surface area. Hence, current chapter on g-C3N4 mainly focuses on basics, properties, and fundamentals of its synthesis and its applications with an aim to improving its photocatalytic performance. In this chapter, the background of photocatalysis, mechanism of photocatalysis, and the several researches on the heterostructure graphitic carbon nitride (g-C3N4) semiconductor are discussed. This research gives a useful knowledge on the heterostructure g-C3N4 and their photocatalytic mechanisms and applications. Finally, the challenges and future research directions of g-C3N4 photocatalysts are summarized to promote their environmental applications. The advantages of the heterostructure g-C3N4 over their precursors are also discussed. The conclusion and future perspectives on this emerging research direction are given.

Keywords: Graphitic carbon nitride (g-C3N4), Photocatalysis, Pollutant degradation, Semiconductors

INTRODUCTION

Carbon nitrides are compounds that contain carbon and nitrogen as major elements with the general chemical formula C_3N_4. In these compounds, carbon atoms are fourfold sp^3 bonded with nitrogen atoms in a regular tetrahedron and then it is connected by other nitrogen atoms having a planar structure, thereby forming a sp^2 bond (Gao et al., 2004). g-C_3N_4 is a polymeric material composed of tris-triazine-based patterns with the C/N ratio=3/4 and small

amount of H. Since it exhibits a stacked structure, g-C_3N_4 is often considered as sp^2-hybridized nitrogen-substituted graphene. Among ultrathin 2D nanomaterials, layered structure graphitic carbon nitride (g-C_3N_4) is analogous to graphite, and its crystal structure is often deemed to be N-substituted graphite structure which formed the sp^2-hybridization of nitrogen and carbon atoms. It has been fabricated by high-temperature polycondensation of different nitrogen-rich precursors, such as melamine, urea, thiourea, dicyandiamide and cyanamide, and the obtained products also show different band gap and specific surface area (Sun et al., 2013).

The compound was first synthesized by the researchers Berzelius and Liebig; they prepared a polymer of triazine (C_3N_3), which is a derivative of carbon and nitrogen and called the prepared compound "melon." Compounds such as melamine, urea, thiourea, cyanamide, and di-cyandiamide when subjected to temperature above 360°C will result in the formation of a three-component heptazine-based melem (triamino-tri-s-triazine, triamino-heptazine, and C_6N_7 $(NH_2)_3$ complex). When this melem is condensed above 520°C, it results in the poly (amino-imino) heptazine $[C_6N_7(NH_2)(NH)]n$ units known as Liebig's adduct "melon" (Chan et al., 2002). g-C_3N_4 is polymeric in nature, metal free, and composed of covalently bonded earth-abundant carbon and nitrogen atoms arranged in a conjugated layer structure. The strong covalent bonds impart both chemical and thermal stability, and the unique delocalized conjugated structure leads to appreciable electronic conductivity in g-C_3N_4 (Zhou et al., 2013) (Fernandes et al., 2015). The focus on g-C_3N_4 started in 2006 with its application as a heterogeneous catalyst for the Friedel–Crafts reaction (Nicollian, 1971). It gained further momentum after Wang et al. reported its application in H_2 generation via visiblelight photocatalytic water splitting (Mishra et al., 2015). Its application as a photocatalyst is further supported by the convenient position of its conduction band (CB) and valence band (VB) at~ – 1.3 V and + 1.4 V, respectively, versus NHE at pH 7.0 which provides thermodynamic feasibility for the redox reactions needed for photocatalytic reactions to occur(Zhou, 2013). Peng et al. reported in 2013 that g-C_3N_4 is also useful for photoreduction of CO_2.

Currently, a voluminous literature is available on the many applications of g-C_3N_4 and its various composites. Composites of g-C_3N_4 with other semiconductors and also foreign element-doped g-C_3N_4 have been explored as the pristine graphitic carbon nitride has a few shortcomings which prove detrimental to its application as a photocatalyst (Mandal, 2011). The most notable among them are fast recombination of charge carriers, inadequate specific surface area, slow surface kinetics, and also partial solubility in water which makes separation a cumbersome process and leads to secondary pollution. In the last couple of years, various reviews pertaining to g-C_3N_4 and its composites have discussed its application in areas of photocatalysis, solar energy conversion, CO_2 photoreduction, and environmental remediation (Bhattacharya et al., 2017). However, there is not much information on its application in electrochemical energy storage, bacterial disinfection, N_2 fixation, and organic synthesis.

Recent research trend on g-C_3N_4 photocatalyst from the "Web of Science" database is displayed in **(Figure 1)** The search was conducted using the keywords "g-C_3N_4" and "photocatalysis", which generated a total of 5462 articles in 2009–2021. When "water" was added as another keyword, the number of searched articles was 3130. The results were classified by year. We can see that g-C_3N_4 has been receiving increased attention for water treatment in the past decade. Fewer than five articles were published before 2011, and then the number increased significantly from 2012, and reached 771 articles in 2021.

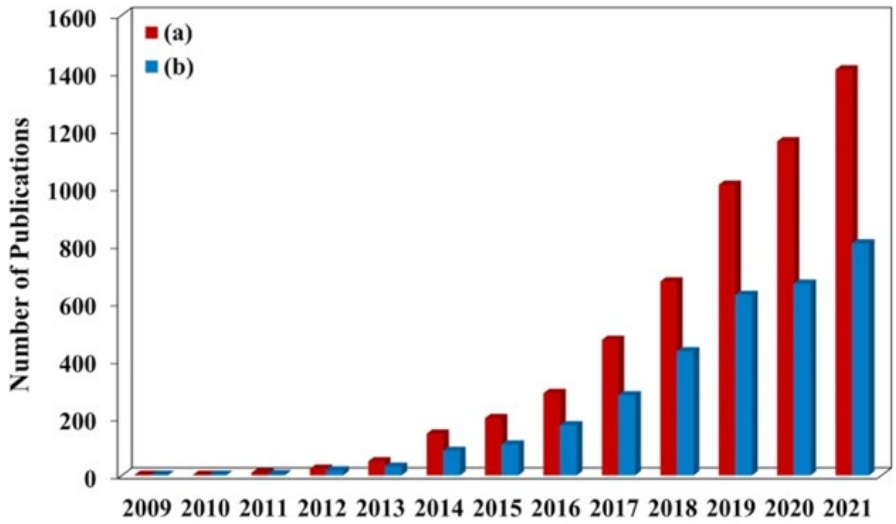

Figure 1. A number of annual publications using "g-C3N4" and "photocatalyst" as keywords; b Number of annual publications using "g-C3N4", "photocatalyst", and "water" as keywords. (Obtained from the "Web of science").

Besides, it presents high thermal and chemical stability, low toxicity, and high solubility in water. The main features of C_3N_4 in the environmental field, namely, potential capacity to adsorb different pollutants and PC activity to degrade them, are mainly derived from its structure. C3N4 is a metal-free organic polymer that has a low production cost through facile synthesis routes.

Carbon nitrides (C_3N_4) are renowned organic semiconductors with a band gap of 2.7 eV, which are connected via tri-s-triazine-based forms. Compared to the different existing carbon materials, C_3N_4 possess hydrogen-bonding motifs, basic surface functionalities owing to the presence of nitrogen (N) and hydrogen (H) atoms, and electron-rich properties. Therefore, carbon nitride is considered a potential candidate for carbon supplementation in material applications.

The discovery of graphitic carbon nitride (g-C_3N_4) as a semiconductor photocatalyst to utilize solar energy for environmental remediation has gathered great attention in the past decade. With a suitable band gap of 2.7 eV that allows it to operate in the visible-light range, high physiochemical stability, appealing electronic band structure, appropriate optical absorption, and ''earth-abundant'' nature allowing economic feasibility, g-C_3N_4 comes as an excellent metal-free photocatalyst for solving the energy crisis and offers a wide range of applications. The porous microspheres showed reduced band gap, enhanced visible-light absorption, and suppressed recombination rate of charge carriers. The aforementioned researches clearly demonstrate the tremendous merits that g-C_3N_4 offers when engineered in terms of its morphology, structure, and porosity and serves as an ideal material for photocatalytic applications.

Compared to the different existing carbon materials, C_3N_4 possess hydrogen-bonding motifs, basic surface functionalities owing to the presence of nitrogen (N) and hydrogen (H) atoms, and electron-rich properties. Therefore, carbon nitride is considered a potential candidate for carbon supplementation in material applications. Hence, many researches on g-C_3N_4 mainly focus on improving its photocatalytic performance.

As a fascinating conjugated visible-light-responsive polymeric semiconductor photocatalyst, g-C_3N_4 has been widely studied as highly efficient photocatalysts or co-catalysts for hydrogen generation, CO_2 conversion and pollutant removal. As is well known, similar to most individual photocatalysts, bulk g-C_3N_4 shows low quantum efficiency because of the fast recombination rate of photoexcited charge carriers and low visible light absorption range, which greatly limits its practical applications.

To date, considerable effort had been devoted to improving the photocatalytic efficiency of this promising photocatalyst and various modification strategies have been proposed, including nanostructure amelioration , metal or nonmetal element doping, formation of g-C_3N_4-based semiconductors hybrids and decoration with a functionalized material. Among those mentioned above, constructing g-C_3N_4-based semiconductors heterogeneous hybrids with suitable band gap semiconductors is a frequently used approach to accelerate the migration of photoinduced charge carriers and inhibit their recombination, and various kinds of g-C_3N_4-based heterojunction hybrids have been constructed by combining g-C_3N_4 with other p-type or n-type semiconductors, such as MoS_2/g-C_3N_4 , CdS/g-C_3N_4, WO_3/g-C_3N_4 and Bi_2MO_6/g-C_3N_4. However, most of these heterojunction nanocomposites need to take into account the matching of energy band structure and the stability of the heterojunction. In addition, integrating with other semiconductors will inevitable introduce the metal elements.

Nitrogen-rich precursors including urea, thiourea, dicyandiamide, melamine, etc. are usually used for the synthesis of g-C_3N_4 by the thermal polymerization method. The morphology of g-C_3N_4 is similar to graphite which shows a two-dimensional layered microstructure. The tri-s-triazine structure of g-C_3N_4 is the most stable phase, which is regarded as the typical formation of g-C_3N_4. The π-conjugated structure of g-C_3N_4 is sp^2-hybridized by carbon and nitrogen. The ideal C/N molar ratio of g-C_3N_4 is 0.75, but most reported g-C_3N_4 is rich with defects, and the C/N molar ratio is close to 0.75, which makes it more activated in catalysis. The elements C and N are earth-abundant, resulting in low-cost preparation. A small amount of hydrogen of amine groups existed in g-C_3N_4. The surface defects and hydrogen are important in photocatalysis, which can serve as surface active sites for reactants adsorption and photocatalysis. The bandgap of g-C_3N_4 is around 2.7 eV with the conduction band (CB) and valence band (VB) potentials at ca. -1.1 eV and 1.6 eV, respectively, resulting in the visible light driven photodegradation.

However, pristine g-C_3N_4 has some disadvantages, including a narrow visible-light response range, small surface areas, and a low separation rate of electron–hole pairs. However, in terms of its practical applications, g-C_3N_4 still has limitations, including poor photoexcited charge separation, limited range of visible light absorption, and low surface areas. All these adverse factors significantly reduce photocatalytic efficiency. To enhance the applications of g-C_3N_4 in photocatalysis, various ways have been developed to improve its abilities for light adsorption and transfer of electron–hole pairs, including morphology control, the introduction of defects, doping with other atoms, coupling with metal, semiconductor, and carbonaceous materials. The excellent properties of these materials are a great impetus to research efforts to explore practical applications and modification methods **(Figure 2).**

To date, there are many photocatalytic applications of g-C_3N_4 in wastewater treatment, including removal of dyes, antibiotics, phenols, etc. More importantly, future areas of

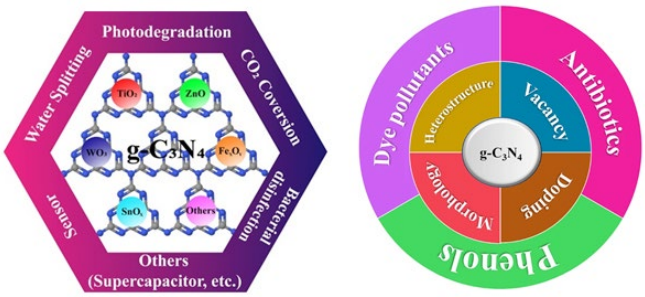

Figure 2. Applications and modification methods of g-C3N4 nanocomposites-based photocatalysts.

research which can be in focus have been discussed with an aim to explore the versatility of g-C_3N_4.

Structure and characterization methods for heterostructure g-C_3N_4

Carbon nitride, C_3N_4, reveals various crystalline forms/ structures such as graphitic-C_3N_4 (g-C_3N_4), cubic-C_3N_4, defect zinc blende-C_3N_4, β-C_3N_4, and α-C_3N_4. Among these structures, g-C_3N_4 exhibits a layered geometry that is analogous to graphite. If the N/C ratio is < 1, the carbon nitride is called N-doped C_3N_4 that contains C atoms as the main phase in which the N atoms are substituted by C atoms and/or bound as N-comprising functional groups onto the C atoms. On the other hand, if the N/C ratio is > 1.0, the carbon nitride is usually named N-rich C_3N_4. g-C_3N_4 displays exceptional physicochemical features as it has the s-triazine core though its electrochemical and electrical properties are restricted by its rather low conductivity.

Among the several allotropes, the graphitic CN (g-CN) has similar carbon network and sp^2 conjugated π structures as a grapheme formed by triazine or tri-s-triazine units cross-linked by trigonal nitrogen atoms to form extended networks that build stacked layers, as shown in **(Figure 3)**. The proportion of triazine or tri-s-triazine units depends on the raw materials used and on the condensation process during the synthesis. Besides, g-CN can present residual hydrogen in defects and different surface terminations such as Brønsted and Lewis basic sites, which confers different chemical properties to the material.

The strong covalent bonds between carbon and nitrogen atoms provide high chemical and thermal stability of g-CN, preventing its photocorrosion under visible light and improving its catalytic activity. Moreover, the porous body and large surface constituted by sp^2 π-conjugative moieties and primary/secondary/tertiary amines improve the adsorbent–adsorbate affinity through π–π electron coupling, covalent, electrostatic, and hydrogen bonds adsorbate/adsorbent interactions, increasing the g-CN pollutant removal performance. The π-conjugated structure is also responsible for the optical properties of CN, which is considered a semiconductor with a bandgap between 1.5 and 2.70 eV, a very desirable characteristic for applications in photocatalysis processes. This property favors the collection

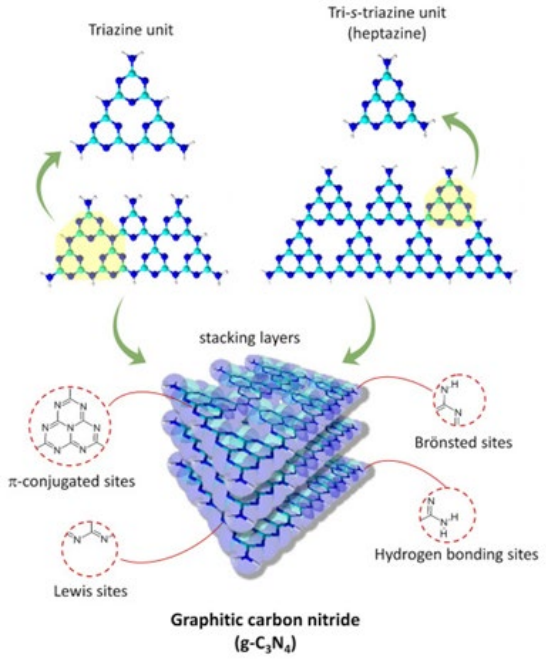

Figure 3. g-CN and its unique graphitic π-conjugated stacking 2D structures and terminal groups. g-CN, graphitic carbon nitride.

of low-energy visible photons (460–827 nm) allowing the execution of PC procedures in a configuration similar to the natural environment.

Structure of g-C_3N_4

Carbon nitrides have different types of polymorphs such as α-C_3N_4, β-C_3N_4, cubic C_3N_4, pseudocubic C_3N_4, and graphite C_3N_4. It is essential to know that in general, C_3N_4 occurs in seven phases, which are α-C_3N_4, β-C_3N_4, cubic C_3N_4, pseudocubic C_3N_4, g-h triazine, g-o triazine, and g-h heptazine. The corresponding band gaps for these phases are 5.5 eV, 4.85 eV, 4.3 eV, 4.13 eV, 2.97 eV, 0.93 eV, and 2.88 eV, respectively. **(Figure 4)** presents the structure of different polymorphs of carbon nitride. Among the polymorphs of carbon nitrides, β-C_3N_4 was found to have hardness and compressibility comparable to that of diamond.

Among all these phases, the most energetically favoured and stable phase was found out to be the tri-s-triazine/ heptazine-based g-C_3N_4 at ambient conditions, and the basic units that established the allotropes of g-C_3N_4 were the triazine (C_3N_3) and heptazine (C_6N_7) rings. Hence, the structure of g-C_3N_4 possesses a layered morphology like graphite, where the heptazine or triazine subunits in the individual layers are connected through tertiary amino groups that cause larger periodic vacancies in g-C_3N_4 and arrange themselves in honeycomb-like structure of two-dimensional (2D) sheets. Recent studies have emphasized that tri-s-triazine **(Figure 5)** forms the basic building unit of g-C_3N_4 since it has high stability. Weak van der Waals force holds the sheets together while the intraplanar bonding is covalent in nature. The ideal nitrogen content in g-C_3N_4

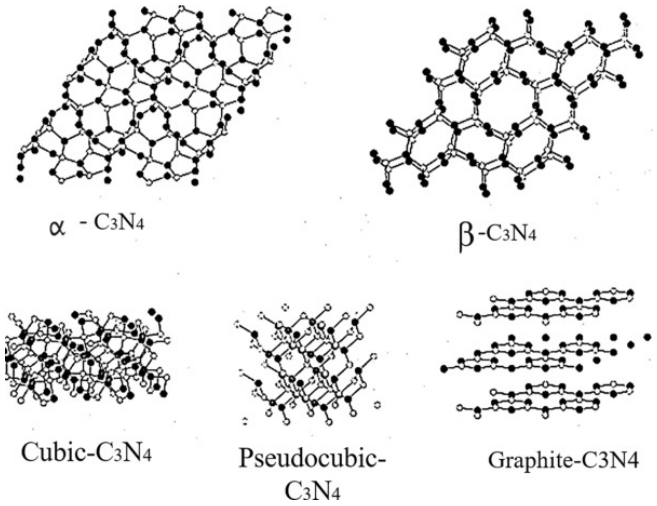

Figure 4. Different polymorphs of carbon nitride.

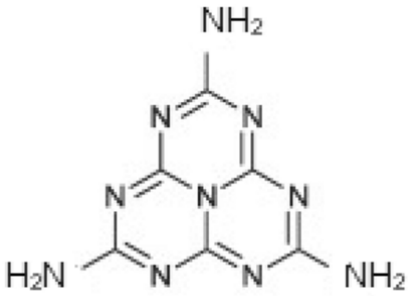

Figure 5. Structure of tri-s-triazine.

is 57.1 at% where the three N species in its structure include graphitic-N, pyridinic-N, and bridge-N. Considering the stacking, it is worthy to note that g-C_3N_4 exhibits stronger binding between the layers and charge transfer perpendicular to the planes in comparison to graphite. This is mainly because of the improved packing density of g-C_3N_4 which is caused by the lowered stacking distance of 0.319 nm between the g-C_3N_4 aromatic layers in comparison to that of graphite (0.335 nm). The three-dimensional (3D) crystal structure of g-C_3N_4 was explored by Fina et al. by X-ray diffraction (XRD) and neutron scattering strategies. They basically employed various structural models and compared their respective XRD patterns to the measured one and then selected the possible model that best described the 3D structure of g-C_3N_4. As a result, they found that the layers of tri-s-triazine units exhibited A-B stacking along with some misalignment of the layers that was favoured because of the reduced π-π repulsive interlayer interactions. The nitrogen in tri-s-triazine units is endowed with lone pair of electrons, and this along with the 2D layer structure of g-C_3N_4 with associated π electrons renders special electronic features to it. The lone pair of nitrogen plays an important role in the electronic structure of g-C_3N_4 because it contributes to the band structure by forming a lone pair valence band, and along with the π bonding electron states, it stabilizes the lone pair state. Hence, the electronic structure of g-C_3N_4 is greatly influenced by the role played by nitrogen lone pairs in it. However, a lot more detailed research is needed to elucidate the electronic structure of g-C_3N_4 thoroughly **(Figure 6)**.

From Doktor, G. (2018). Utilization of graphitic carbon nitride in dispersed media.

As shown in **(Figure 7a)**, it is generally believed that the structure of g-C_3N_4 is composed of tri-s-triazine units. Furthermore, as shown in **(Figure 7b)**, carbon nitride has a bandgap of about 2.7 eV, making it responsive to visible light. The band structure of carbon nitride endows it with excellent redox potential, which satisfies the potential for most photocatalytic CO_2 reactions . More importantly, carbon nitride can form a two-dimensional/two-dimensional (2D/2D) heterojunction with GO via π–π conjugation, which is considered as an ideal heterostructure for charge carrier transport . Therefore, carbon nitride/GO composites have been extensively studied in photocatalytic CO_2 reduction.

Morphology

The morphological structure of the synthesized photocatalyst plays a significant role in its photocatalytic activity. SEM, TEM, and XRD are used to study the morphology of the as-prepared photocatalyst. XRD shows different peaks that confirm that the formed structures are in agreement with the standard cards. SEM and TEM show the morphology of the as-prepared photocatalyst. **(Figure 8a)** shows the XRD spectra of g-C_3N_4 (h), Bi_2MoO_6 (a), and the g-C_3N_4/Bi_2MoO_6 composites (b–g). As seen, the peaks at 27.40° and 13.04° are corresponding to the (002) and (100) planes of g-C_3N_4 while the peaks at 28.3°, 32.6°, 47.7°, and 55.4° are in agreement with (131), (002), (060), and (331) planes of Bi_2MoO_6, respectively which shows the perfect formation of the g-C_3N_4/Bi_2MoO_6 composite. The existence of a uniform fringe interval (0.336 nm) in the TEM images **(Figure 8b)** is in agreement with the (002) lattice plane of g-C3N4 while that of 0.249 nm is in agreement to the (151) lattice plane

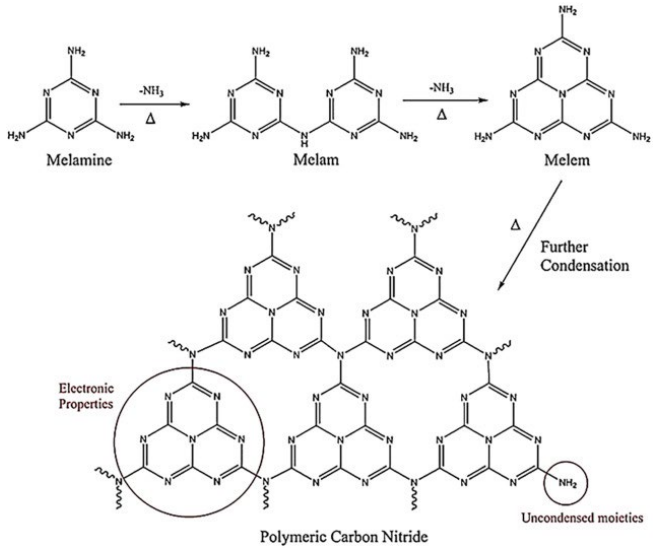

Figure 6. Pictorial representation of polymeric carbon nitride.

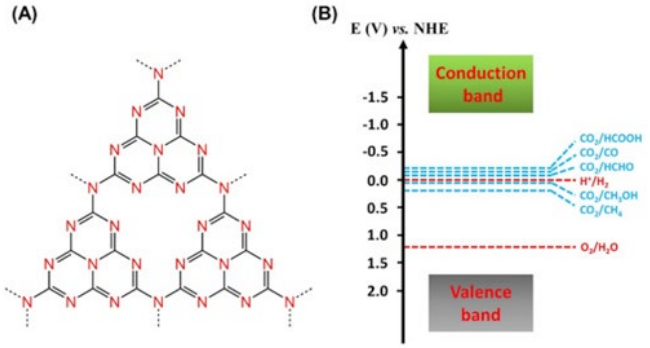

Figure 7. (A) Molecular structure and (B) energy band position of g-C3N4 .

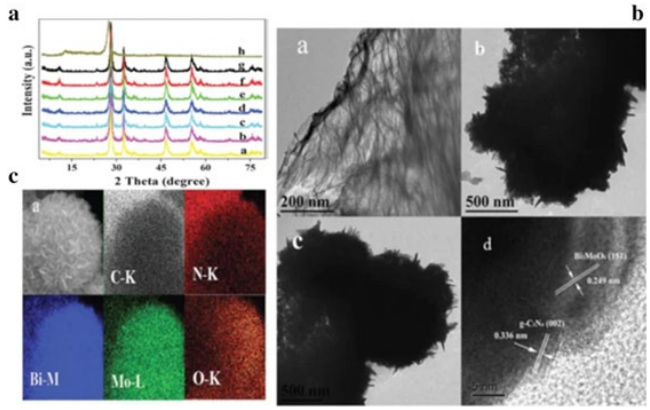

Figure 8. (A) XRD of (b–g) g-C3N4/Bi2MoO6 composites with different g-C3N4 content (a) Bi2MoO6 (h) g-C3N4 (B) TEM images of (a) g-C3N4 (b) Bi2MoO6 (c)g-C3N4/Bi2MoO6 composite (C) SEM image of (a) g-C3N4/Bi2MoO6 showing corresponding elemental (C, N, Bi, Mo, and O) mapping reproduced with permission. Copyright 2014 royal society of chemistry.

of Bi_2MoO_6. In the same shape **(Figure 8c)** ascribed by the elemental mapping of C-K, N-K indicates the existence of g-C_3N_4 while the mapping of Bi-M, Mo-L, and O-K shows the existence of Bi_2MoO_6 in the as-prepared heterojunction. This proves that there were the perfect formation of the heterojunction between g-C_3N_4 and Bi_2MoO_6.

X-ray photoelectron spectroscopy (XPS) characterization

The sp^2-bonded carbon in N-containing aromatic rings (N–C=N) **(Figure 9a)** were ascribed to the C 1s signals at 288.2 eV while sp^2-hybridized aromatic nitrogen bonded to carbon atoms (C=N–C) in triazine rings was attributed to 398.8 eV. This confirms the presence of sp^2-bonded graphitic carbon nitride. The existence of peaks at 159.4 and 164.5 eV is caused by Bi^{3+} in BiOCl while the peak at 530.2 eV is attributed to the Bi–O bonds in $(BiO)^{2+}$ of the BiOCl. The weak peak at 404 eV is caused by the fact that g-C_3N_4 is coupled with BiOCl through the p-electrons of CN heterocycles. This confirms the coexistence of g-C_3N_4/BiOCl composite.

It has been reported that the photocatalytic activity of g-C_3N_4/Bi_2MoO_6 (A8) was higher than those of g-C_3N_4 and Bi_2MoO_6, where about 98% of RhB was removed by g-C_3N_4/Bi_2MoO_6 composite, while less than < 60% was removed by pure g-C_3N_4 (A0) or Bi_2MoO_6 as seen in **(Figure 9b,c)**

Synthesis and structural modification of carbon nitride

Graphitic carbon nitride (g-C_3N_4-) is a robust, metal-free, abundant, non-toxic polymeric semiconductor that can be easily synthesized via one-step thermal treatment using readily available nitrogen-rich precursors like cyanamide,

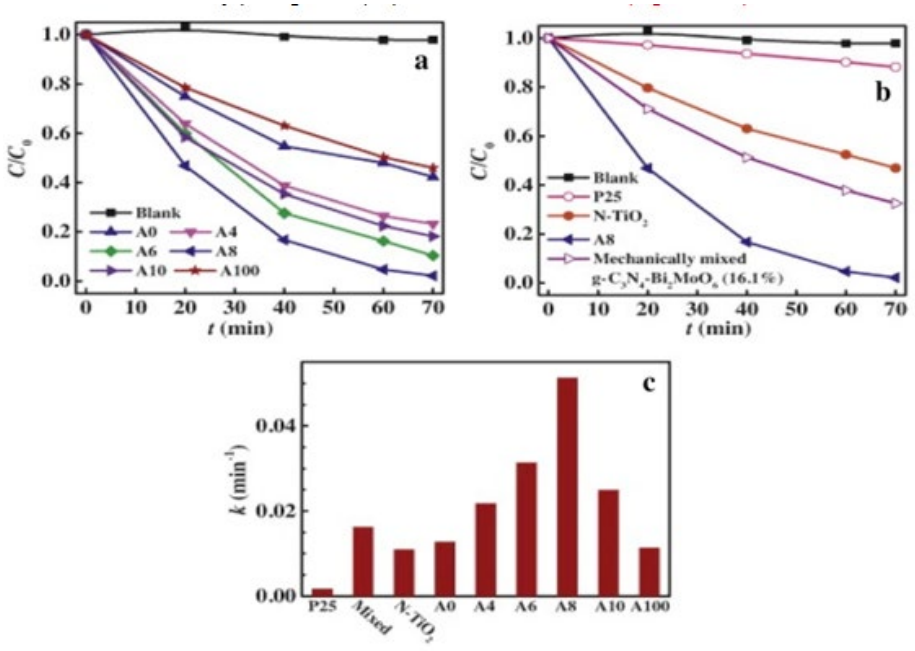

Figure 9. a, b RhB degradation over various photocatalysts and c corresponding rate constants (k) reproduced with permission. Copyright 2014 Elservier B.V.

urea, thiourea, melamine, and dicyandiamide. There are reports on synthesis of g-C_3N_4 from less common precursors like guanidine thiocyanate and guanidinium chloride .

The common techniques methods that have been effectively used for the synthesis of g-C_3N_4 for its various applications mainly include thermal condensation, solvothermal, chemical vapour deposition, microwave heating, sol–gel synthesis, physical vapour deposition, and hydrothermal approach. The thermal polymerization method is the most common method.

In general, g-C_3N_4 is easily synthesized by thermal polymerization of nitrogen-rich precursors including urea , melamine, dicyandiamide , cyanamide , and thiourea at different temperatures. **(Figure 10)** shows the temperature and atmosphere for preparing g-C_3N_4 from different precursors.

However, if the sulphur atoms in thiourea has been replaced with oxygen and, thus, employ urea as the precursor for g-C_3N_4 synthesis, it can yield exceptionally enhanced g-C_3N_4 with high surface area and porous structure as it has been realized in recent years. As an instance, Zhang et al. prepared g-C_3N_4 by utilizing urea as a precursor without the use of any hard or soft template and suggested a microscopic mechanism for the reaction pathway of g-C_3N_4 **(Figure 11)**. The nanoporous g-C_3N_4 displayed a high Brunauer–Emmett–Teller (BET) surface area of 69.6 m^2 g^{-1} and enhanced photocatalytic activity towards H_2 production by water splitting, which was 3.1 and 2.26 times the activity of thiourea-derived g-C_3N_4 and dicyandiamide-derived g-C_3N_4, respectively. The heat of polymerization was lower in the urea precursor compared to that of thiourea due to stronger electronegativity of O atom compared to S which led to stronger hydrogen bonds in the former. Also, the release of H_2O after reaction with self-supported NH_3 was decelerated due to higher bond energy of C–O compared to C–S bonds which reduced the extent of polymerization and led to the formation of more porous g-C_3N_4 with higher BET surface area.

Sulfur-mediated synthesis has been developed to modify the texture, optical and electronic properties, as well as the photocatalytic functions of a carbon nitride semiconductor. The water oxidation reaction has been achieved at a moderate rate with only photocatalysts without the aid of co-factors.

The nanostructure design of g-C_3N_4, like nanowires, nanorods, nanotubes, or two-dimensional (2D) nanosheets, has an exceptionally high specific surface area, maximum light absorption, and improved charge separation. A viable approach towards tuning the porosity, structure, morphology, surface area, and size is by the templating method which can be reviewed as 'hard' or 'soft' **(Figure 12)**.

The g-C_3N_4@TiO_2 core-shell structure photocatalysts with controlled ultrathin g-C_3N_4 layer (0 nm, 1.0 nm, 1.5 nm, 3.0 nm) were prepared by a new method of the sol-gel approaches in situ coating re-assembled. The g-C_3N_4@TiO_2 sample with 1.0 nm thickness of shell layers has the highest visible light photocatalytic degradation phenol activity which is almost 7.2 times as high as that of bulk g-C_3N_4. The highest photocurrent response intensity is increased by ten times higher than that of g-C_3N_4 and five orders of magnitude compare to TiO_2. The removal rate of phenol using g-C_3N_4@TiO_2 core-shell catalyst is 30% and the degree of mineralization by the same catalyst is 19.8%, which dramatically increase compared with that of g-C_3N_4 and TiO_2. The enhanced performance of the degradation phenol and the mineralization is owing to effective charge separation revealed by the photoluminescence (PL), electrochemical impedance spectroscopy (EIS) and density functional theory calculations (DFT), superoxide radicals as the main oxidative species proved by electron spin resonance spectroscopy (ESR). And the core-shell structure could effectively promote the electron transfer from g-C_3N_4 to TiO_2 during the catalytic

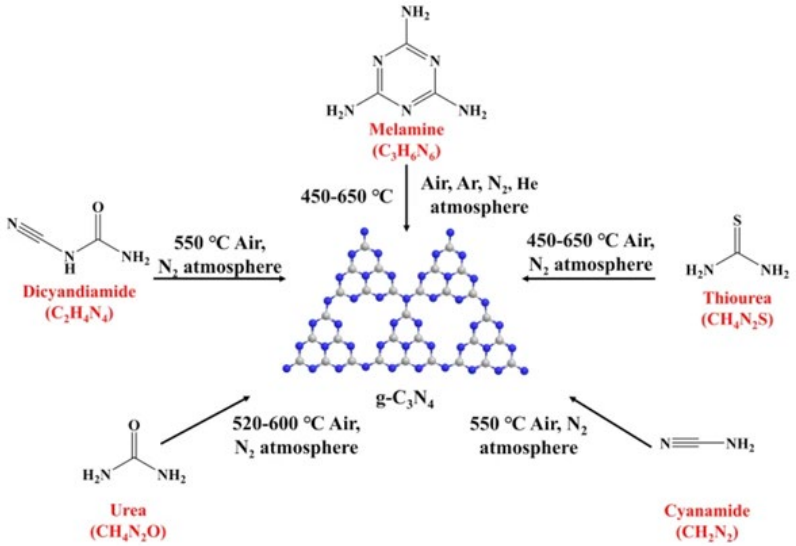

Figure 10. Preparation of g-C_3N_4 from different precursors.

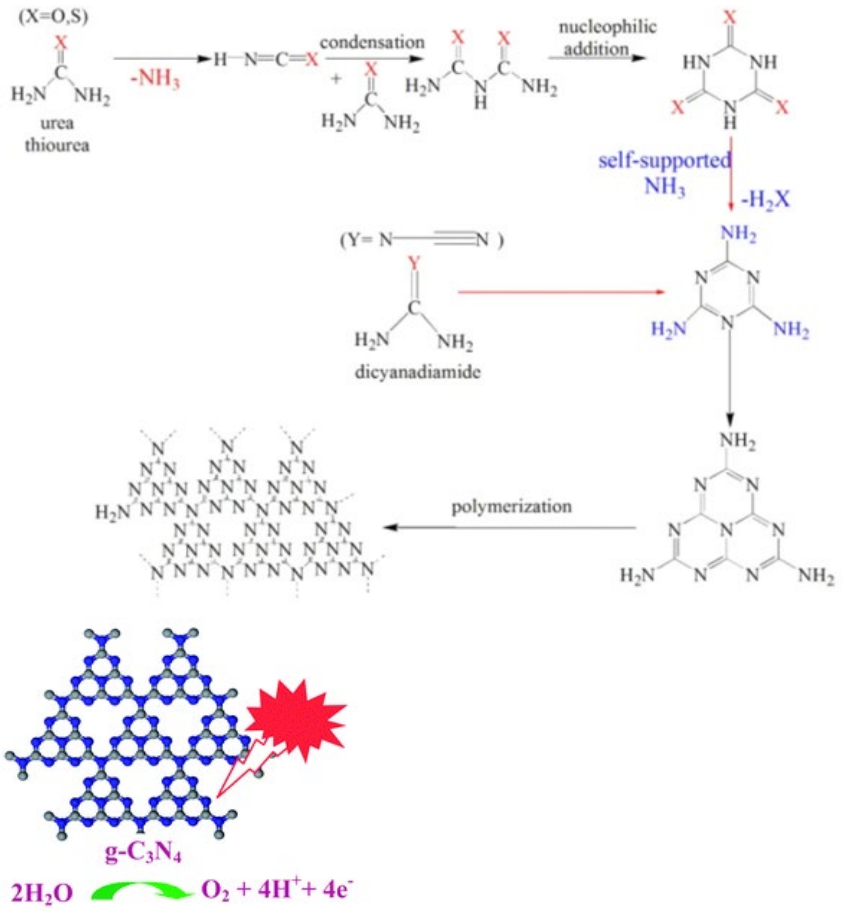

Figure 11. Reaction pathway for formation of g-C_3N_4 using urea/thiourea as precursor. (Reproduced from ref with permission from the royal society of chemistry).

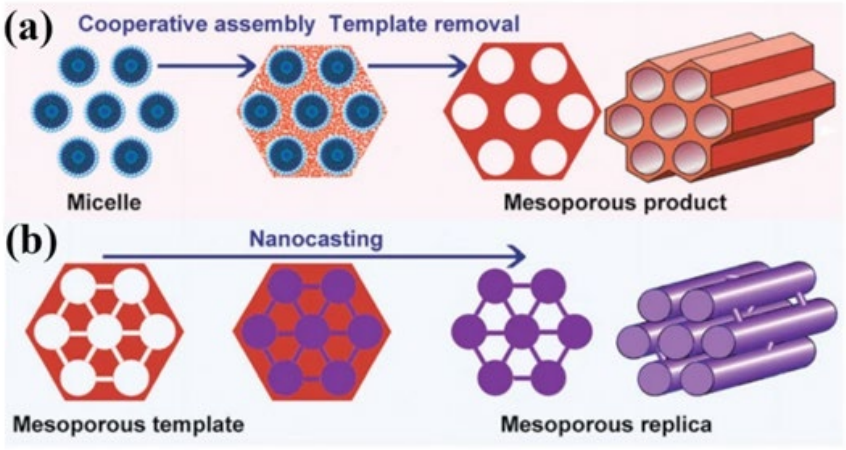

Figure 12. Representation of the synthesis route for ordered mesoporous materials by: a soft-templating method, and b hard-templating method. (Reproduced from ref with permission from the royal society of chemistry).

process. The results of repetitive experiment and cycle experiment show that the g-C_3N_4@TiO_2 has a strong binding force between the core and shell, which is stable, without secondary pollution and convenient for recovery. What's more, the results revealed the law between the different g-C_3N_4 shell layers (0 nm, 1.0 nm, 1.5 nm, 3.0 nm) over the g-C_3N_4@TiO_2 samples and the corresponding catalytic activity, which successfully established the structure-activity relationship. A new catalytic concept namely layer-dependent effect was found **(Scheme 1)** , which is number of layers over g-C_3N_4 of the core-shell structure determines photocatalytic activity.

Holey graphitic carbon nitride (HCN) with highly enhanced photocatalytic reduction activity has been prepared by one-

step thermal polymerization of hydrothermal product of melamine and then loaded with Ni/MoO_2(NiMo) cocatalyst obtained by $NaBH_4$ reduction process as shown in **(Scheme 2)** The obtained material was used for photocatalytic production of H_2 from water reduction and H_2O_2 production from O_2 reduction. The best photocatalyst (1% NiMo/HCN) exhibited a H_2 evolution rate of 8.08 µmol/h while no H_2 was detected over 1% NiMo-modifed bulk g-C_3N_4(BCN) under visible light illumination. Moreover, this rate is 1.7 times higher than that of 1% Pt-modified HCN. The 1% NiMo/HCN catalyst also exhibited the highest H_2O_2 production activity with a value of 6.13 µmol/h. Such enhancement was ascribed to the efficient charge carrier separation and migration, which were promoted by the large specific surface area and pore volume of HCN and the synergy between MoO_2 and Ni. The proposed method to obtain HCN is expected to open up new ways in development of highly-active HCN-based photocatalysts for photocatalytic reduction reactions.

Changing the morphology of the synthesized photocatalysts plays a significant effect in its photocatalytic activity. Optical, electronic, mechanical, magnetic, and chemical properties of carbon nitride materials are highly dependants on the change of size, composition, dimension, and shape. Hard and soft templating methods, template-free methods, and exfoliation strategies are among the methods used to modify the structure of the synthesized carbon nitride photocatalysts. Templating modifies the physical properties of carbon nitride semiconductor materials by varying morphology and introducing porosity. Template-free method creates vacancies in carbon nitride photocatalysts resulting to introduction of additional energy levels or acting as reactive sites, and thus profoundly changing the overall photocatalytic activity. Exfoliation modifies the bulky carbon nitride into nano-sheet carbon nitrides which increase the surface area for active sites, hence increasing its photocatalytic activity. Also, carbon nitride can be modified into nano-rods and nanotubes which all have effects on the photocatalytic activity of the synthesized photocatalyst.

Modification with other carbonaceous materials

Carbonaceous materials have a wide range of physical and chemical properties derived from the spatial organization of carbon atoms and their chemical covalent bonds. Carbonaceous materials such as carbon nanotubes (CNTs), multi-walled carbon nanotubes (MWCNTs), carbon dots (CDs), graphene, and reduced graphene oxide have been widely incorporated in modifying different photocatalyst semiconductors in order to enhance their photocatalytic activity. Ma et al. reported the synthesis of an artificial Z-scheme visible light photocatalytic system using the reduced grapheme oxide as an electron mediator. In their report, results showed that g-C_3N_4/RGO/Bi_2MoO_6 exhibited high photocatalytic activity (k = 0.055 min^{-1}) over degradation of rhodamine B dye as one of the common pollutant. Also, in 2017, Ma and coworkers reported the synthesis of Bi_2MoO_6/CNTs/g-C_3N_4 with enhanced debromination of 2, 4-dibromophenol under visible light. The composite resulted into higher photocatalytic activity (k = 0.0078min^{-1}) which was 3.61 times of g-C_3N_4 (k = 0.00216 min^{-1}).

Heterostructure graphitic carbon nitride composite

The heterojunctions that are formed between the host semiconductors provide an internal electric field that facilitates separation of the electron–hole pairs and induces faster carrier migration. It involves the combination of two semiconductors to form the heterojunction semiconductors. Several researches have proven that the heterojunction formation is the promising strategy to the improvement of

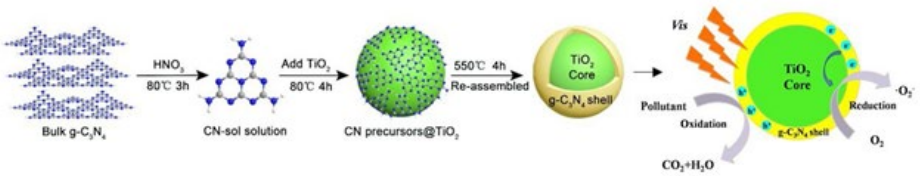

Scheme 1. Photocatalytic activity enhancement of core-shell structure g-C_3N_4@TiO_2 via controlled ultrathin g-C_3N_4 layer.

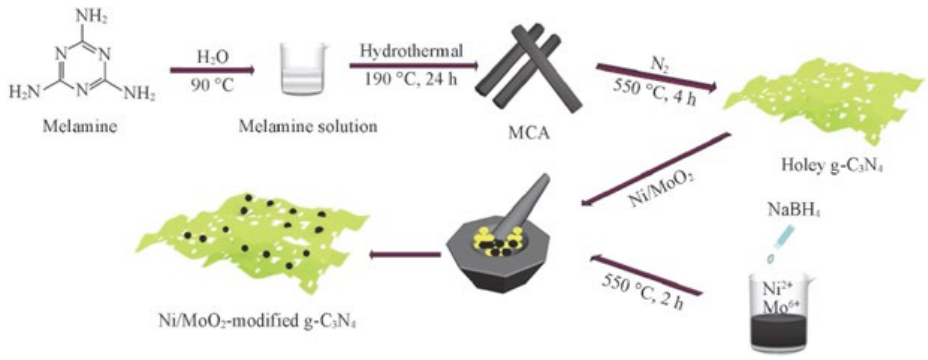

Scheme 2. Schematic representation of the synthesis of NiMo/HCN Photocatalyst.

the g-C_3N_4 photocatalytic activity.

According to the band gap and electronic energy level of the semiconductors, the heterojunction semiconductor can be primarily divided into three different cases: straddling alignment (type I), staggered alignment (type II), and Z-scheme system. The band gap, the electron affinity (lowest potential of CB), and the work function (highest potential of VB) of the combined semiconductors determine the dynamics of the electron and hole in the semiconductor heterojunctions.

Type I heterojunction semiconductor

In type-I heterojunction semiconductor, both VB and CB edges of semiconductor **2** are localized within the energy gap of semiconductor **1**, forming straddling band alignment **(Figure 13)**. The VB and CB alignment play a significant role in the determination of the physical properties of the generated charges and the photocatalytic performance. This kind of heterojunction does not improve photocatalytic activity of the prepared photocatalyst because of the accumulation of both charge carriers on one semiconductor. From, the photogenerated electrons (e^-) are expected to move from the $SrZrO_3$ conduction band (CB) to $SrTiO_3$ conduction band (CB) due to reduction potential differences. Also, the photogenerated holes (h^+) generated in the valence band (VB) of $SrZrO_3$ will migrate to the valence band of $SrTiO_3$ due to the difference in their oxidation potentials.

Hence, both electrons and holes will accumulate in $SrTiO_3$ semiconductor causing high recombination to take place.

Type II heterojunction semiconductor

In type II heterojunction semiconductor reduction and oxidation, reactions occur for semiconductor with a lower reduction potential and semiconductor with a lower oxidation potential, respectively. In type-II heterojunction

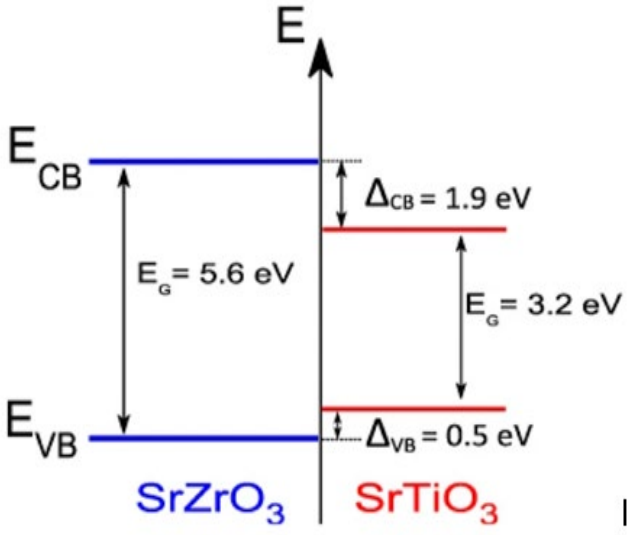

Figure 13. The systematic representation of the type I heterojunction semiconductor.

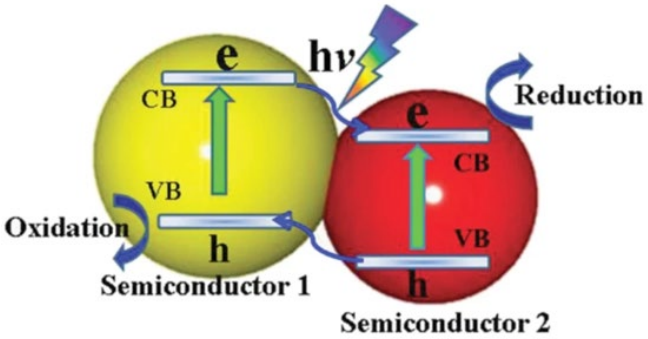

Figure 14. The systematic representation of the type II heterojunction semiconductor reproduced with permission. Copyright 2015 WILEY-VCH Verlag GmbH & Co. KGaA, Weinheim.

semiconductor, both VB and CB of semiconductor **1** are higher than that of semiconductor **2 (Figure 14)**. Electrons from semiconductor 1 migrate to semiconductor **2** while the holes move from semiconductor **2** to semiconductor **1**. If both semiconductors have sufficient intimate contacts, an efficient charge separation will occur during light illumination. Consequently, charge recombination is decreased, and so charge carriers have a longer lifetime, which results in higher photocatalyst activity. Type II heterojunction semiconductor suffer from steric hindrance of charge transfer. When electron in the CB of semiconductor **1** migrates to the CB of semiconductor **2**, there is a repulsion force created between coming electrons and existing electrons. Same applies when holes from the VB of semiconductor **2** migrates to the VB of semiconductor **1**. In the steric hindrance created, there can be a small amount reduction in the expected photocatalytic activity of the as-prepared type II heterojunction photocatalyst.

Z-Scheme heterojunction semiconductor

In the course of development and modifications of visible light-driven photocatalytic systems, Z-scheme was originally introduced by Bard in 1979. The Z-scheme heterojunction was developed to solve the steric hindrance exerted in type II heterojunction. Currently, there are three generations of the Z-scheme photocatalytic system **(Figure 15)**.

First-generation Z-scheme heterojunction

It is also known as liquid-phase z-scheme photocatalytic system. It is built by combining two different semiconductors with a shuttle redox mediator (viz. an electron acceptor/donor (A/D) pair) as seen in **(Figure16a).**

Second-generation Z-scheme heterojunction semiconductor

It is also known as all-solid-state (ASS) Z-scheme system. In order to overcome the obvious problems identified in the first generation, Tada et al. in 2006 have been synthesised the all-solid-state CdS/Au/TiO_2 Z-scheme. An ASS Z-scheme photocatalytic system is composed of two different

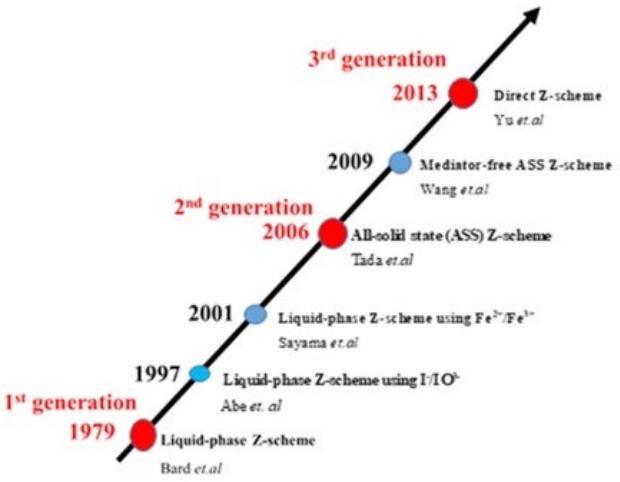

Figure 15. The roadmap of the evolution of z-scheme photocatalytic system reproduced with permission from with slight modifications. Copyright 2017 WILEY-VCH Verlag GmbH & Co. KGaA, Weinheim.

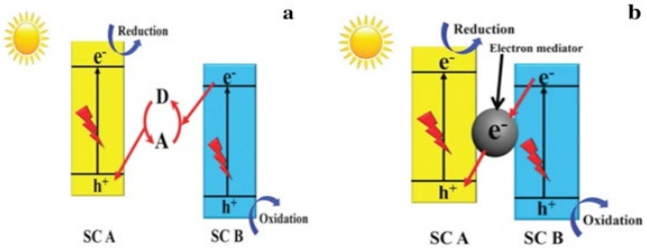

Figure 16. (a) A systematic representation of first Z-scheme generation where A and D are the electron acceptor and donor respectively. (b) A systematic representation of the second-generation Z-scheme (ASS) reproduced with permission. Copyright 2017 WILEY-VCH Verlag GmbH & Co. KGaA, Weinheim.

semiconductors and a noble-metal nanoparticle (NP) as the electron mediator as seen in **(Figure 16b)**. The use of the noble metal solves the backward reaction that was happening in the first generation (liquid-phase Z-scheme). Noble metals are expensive and very rare to obtain causing their wide application to be limited. Also, noble metals have high ability to absorb light. This affects the light absorbance of photocatalytic semiconductors, and their photocatalytic activities are also affected. In solving the light absorbance problem Wang et al. in 2009 synthesised the mediator-free ASS Z-scheme.

Third-generation Z-scheme heterojunction semiconductor

It is commonly known as direct Z-scheme semiconductor. A direct Z-scheme photocatalyst consists of only two semiconductors that have a direct contact at their interface. All the advantaged features in the previous two generation are inherited in direct Z-scheme photocatalyst. Unlike a type II semiconductor, electrons in the CB of semiconductor B migrate to recombine with the holes generated in the VB of semiconductor A forming a Z-transfer as shown in **(Figure 17a, b)**.

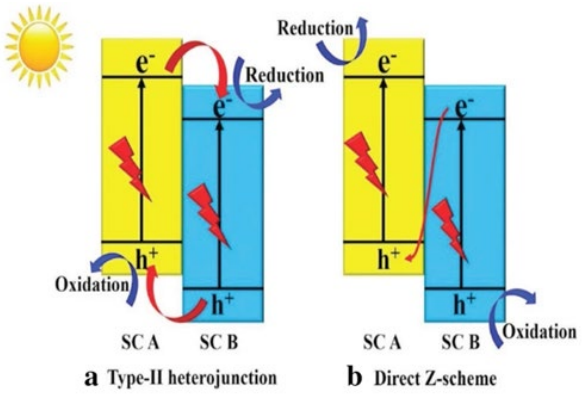

Figure 17. A comparison of the charge transfer between type II heterojunction (a) and Z-scheme heterojunction (b) reproduced with permission. Copyright 2017 WILEY-VCH Verlag GmbH & Co. KGaA, Weinheim.

Presently, g-C_3N_4 is studied as a new-generation photocatalyst to recover the photocatalytic activity of traditional photocatalysts like TiO_2, ZnO, and WO_3. Graphitic carbon nitride (g-C_3N_4) is assumed to have a tri-s-triazine nucleus with a 2D structure of nitrogen heteroatom substituted graphite framework which include p-conjugated graphitic planes and sp^2 hybridization of carbon and nitrogen atoms. Bulky carbon nitride can be synthesized through thermal condensation of nitrogen-rich (without a direct C-C bound) precursors such as cyanamide, dicyandiamide, thiourea, urea, and melamine. Also, it can be synthesised through polymerization of nitrogen-rich and oxygen-free precursors (comprising the pre-bonded C-N core structure) by physical vapour deposition, chemical vapour deposition, solvothermal method, and solid-state reactions. Having the band gap of 2.7 eV and the conduction and valence band position at − 1.4eV and 1.3 eV, respectively, versus NHE (normal hydrogen electrode), g-C_3N_4 have shown great ability to carry photocatalytic activity in the visible light irradiation without the addition of any noble-metal co-catalyst. Apart from visible light utilization, bulky carbon nitride is hampered by high-charge carrier recombination which reduces its photocatalytic activity. Different researchers have studied on the modification of g-C_3N_4 to counteract the challenge of charge carrier recombination and band engineering. Several modifications have been studied over decades including structural modification, doping, modification with carbonaceous and plasmonic material, and heterojunction composite formation. The stability of photocatalysts is crucial for their practical application.

Photocatalytic activities of g-C_3N_4

The fundamental mechanism of the photocatalytic semiconductor depends on the incident light photon with equal or large energy than the band gap energy strike the semiconductor; the electrons in the valence band (VB) are photoexcited and move to the conduction band (CB), leaving equal number of the holes in the valence band (VB). The photoexcited electron (e^-) and holes (h^+) in the CB and VB,

respectively, moves to the surface of the semiconductor. It is at the surface of the photocatalyst semiconductor where reduction and oxidation of the electron acceptor and electron donor, respectively, take place as seen in **(Figure 18)**. The photocatalytic mechanism is summarised by the following Eqs. 1, 2 and 3

1. Semiconductor + hν→ e^- CB + h^+ VB
2. e^- CB + A→A^-
3. h^+ VB + D→ .D+

The doping effect, surface modification, and heterojunction formation have the direct effect on the movement of the generated charge carriers (electron and holes) of the synthesized photocatalyst. When the electron mediator atom is introduced in the semiconductor, the movement of charge carrier depends on whether the mediator is an electron donor or acceptor. The dopant not only controls the charge recombination, but it also assists in band gap engineering of some wide band gape semiconductors. In heterojunction composite photocatalyst, the charge carrier transfer depends on the nature and properties of the participating semiconductors.

It shows how the photocatalysts can be reused without or with little loss in their activities. In order to know the reusability of the photocatalyst, the degradation of the pollutant by the same composite for several times/cycles is performed.

Recently, the photocatalytic applications of g-C_3N_4-based materials in the environment have attracted wide attention. The photodegradation applications of g-C_3N_4-based materials for dye pollutants, antibiotics, and phenols are reviewed. The sources of antibiotics, phenols, and dyes are shown in. So far, g-C_3N_4 has been widely used as an environmental photocatalyst, therefore its photocatalytic degradation mechanism for organic pollutants has been explored. The photocatalytic process can be divided into four stages **(Figure 19)**. Firstly, visible light is absorbed by g-C_3N_4 (Step 1). The light absorption stage is up to the surface morphology and structure of the photocatalyst.

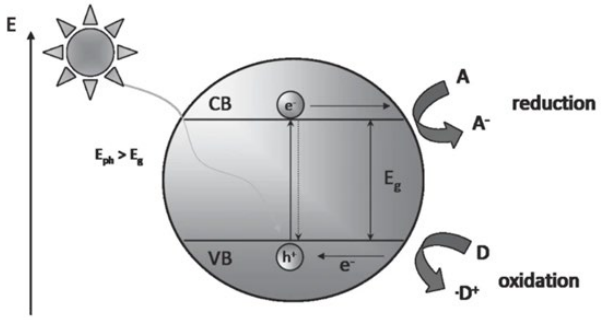

Figure 18. A systematic depiction of the general mechanism of photocatalytic semiconductor reproduced with permission. Copyright 2013 WILEY-VCH Verlag GmbH & Co. KGaA, Weinheim.

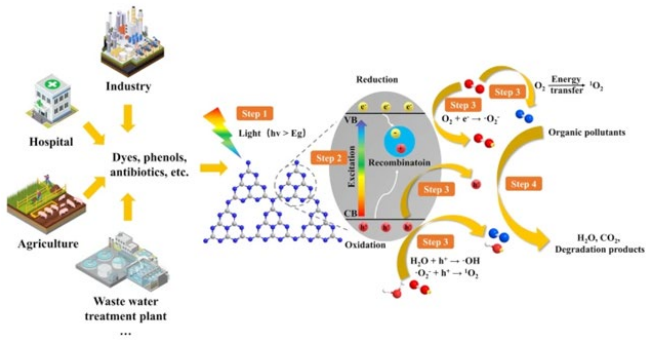

Figure 19. Degradation mechanisms of g-C3N4 for organic pollutants of different sources.

When the energy of light is greater than or equal to the energy of the semiconductor band gap (Eg), the electrons are excited from VB to CB, leaving holes in VB, thus achieving effective separation of photogenerated carriers (Step 2). The band gap of g-C_3N_4 can be further adjusted by doping, introducing defects, etc. thus promoting its use of visible light. At the same time, in order to promote photocatalysis, it is necessary to prevent the recombination of electrons and holes. Furthermore, photogenerated electrons and holes are separated and migrated (Step 3). Photogenerated electrons react with electron acceptors (such as oxygen) to form superoxide groups and holes react with water to produce hydroxyl radicals. Singlet oxygen ($^1O_2$) can be produced by the reaction of holes with superoxide groups or reacting with oxygen by energy transfer. At last, g-C_3N_4 can adsorb the diffused pollutants on its surface, and the active substances degrade them into the water, carbon dioxide, and other products after redox reactions (Step 4). For each target pollutant, the photocatalytic mechanism will be different.

Future of heterostructure g-C_3N_4

The future research of heterostructure g-C_3N_4 nano-based photocatalyst may focus on the design and synthesis of more effective nanostructures, which are responsive to morphology monitoring, evaluating the photocatalysis practicality, and the degradation behavior and mechanism of more types of pollutants, especially for non-dyed pollutants and then exploring the applications of diverse g-C_3N_4 nano-based particles in treating wastewater, its effective application in solar energy utilization, sensing applications by fully assessing their photocatalytic ability, cost, energy consumption, and reusability.

One of the key areas to consider for future studies should mainly focus on employing new technologies or combination of the existing techniques of increasing the settling velocity of g-C_3N_4 to upturn the run-off rate that could be used to improve the material for improving photocatalytic activities.

CONCLUSIONS AND PERSPECTIVES

Recently, graphitic carbon nitride has been the most scientific researched semiconductor due to its narrow band gap of 2.7

eV which permits it to absorb visible light directly without modification. Graphitic carbon nitride (g-C_3N_4) exhibits high thermal and chemical stability, owing to its tri-striazine ring structure and high degree of condensation. Although various graphitic carbon nitride semiconductors have been studied for photocatalytic degradation of pollutants, their photocatalytic performance remains unsatisfactory suffering highly from charge (electron–holes) recombination. To overcome the electron–hole recombination in a single g-C_3N_4 semiconductor, different researchers have made enormous efforts toward developing novel photocatalytic systems with high photocatalytic activities. The development of heterostructured graphitic carbon nitride photocatalysts semiconductors has proven to be potential for use in enhancing the efficiency of photocatalytic pollutant degradation through the promotion of the separation of photogenerated electron–hole pairs and maximizing the redox potential of the photocatalytic system.

In the present chapter, we highlight the basics, properties, synthesis, structural modification fundamentals and applications of g-C_3N_4 and its derivatives in the photodegradation of organic pollutants in water. The g-C_3N_4-based photocatalysts have the advantages of high efficiency, saving energy, and reusability, making them promising photocatalysts for environmental applications, especially with respect to organic pollutant photodegradation. Further investigations thus should be conducted to promote research in this field and fill following important knowledge gaps. 1) Previous studies have mainly concentrated on improving the photodegradation activity of g-C_3N_4-based materials under laboratory experimental conditions. The degradation activity and mechanism for organic pollutants in the actual industrial wastewater are still unclear. 2) The applicability of g-C_3N_4 photodegradation technique under natural conditions needs to be further evaluated. 3) Obstacles have yet to be addressed for the upscale from laboratory to commercially available photocatalytic wastewater treatment technology. 4) Most of the relevant laboratory studies have only focused on the removal of one pollutant at a time. However, it rarely happens in real wastewater, which usually contains various pollutants including both easily degradable and recalcitrant ones.

This chapter place special emphasis on recently researched heterostructure graphitic carbon nitride (g-C_3N_4) looking at their characterizations and their applications in ambient conditions. Although photocatalytic degradation is an ideal strategy for cleaning environmental pollution, it remains challenging to construct a highly efficient photocatalytic system by steering the charge flow in a precise manner. Different researches have proven the high photocatalytic activity of the heterostructured semiconductors over pollutants degradation, hydrogen gas evolution, and carbon dioxide reduction. Among others, heterostructured carbon nitride (CN) semiconductors in recent decades have shown the anonymous photocatalytic activity towards organic pollutants, hydrogen production, and carbon dioxide. Reasonably, g-C_3N_4 has revealed to be one of the best candidates suitable for developing and assembling state-of-the-art composite photocatalysts. Therefore, there is slight doubt that the considerable advancement of g-C_3N_4 nano-based particle will endure to develop in the near future. Hence, more researches should consider its modification structures, mechanisms, and the degradative abilities of this candidate.

Abbreviations list

$^1O_2$	Singlet oxygen
2D	two-dimensional
3D	three-dimensional
A/D	electron acceptor/donor pair
ASS	all-solid-state
BET	Brunauer–Emmett–Teller
CB	conduction band
CDs	carbon dots
CN	carbon nitride
C_3N_3	triazine
C_3N_4	Carbon nitrides
C_6N_7	heptazine
CNTs	carbon nanotubes
DFT	density functional theory
E_g	band gap
ESR	electron spins resonance spectroscopy
***g*-C_3N_4**	graphitic carbon nitride
GO	graphene oxide
H	hydrogen
HCN	Holey graphitic carbon nitride
MWCNTs	multi-walled carbon nanotubes
N	nitrogen
NP	nanoparticle
PL	photoluminescence
QDs	quantum dots
SEM	scanning electron microscopy
TEM	Transmission electron microscopy
VB	valence band
XPS	X-Ray Photoelectron Spectroscopy
XRD	X-ray diffraction

REFERENCES

1. Gao, Xiaohu, Cui, Yuanyuan, Levenson, et al (2004). In vivo cancer targeting and imaging with semiconductor quantum dots. Nature Biotechnology. 22:969-76.
2. Sun, Dong, Ban, Rui, Zhang, et al (2013). Hair fiber as a precursor for synthesizing of sulfur- and nitrogen-co-doped carbon dots with tunable luminescence properties. Carbon. 64:424-34.
3. Chan, Warren CW, Maxwell, Dustin J, Gao, et al (2002). Luminescent quantum dots for multiplexed biological detection and imaging. Current Opinion in Biotechnology. 13: 40-6.
4. Zhou, Juan, Yang, Yong, Zhang, et al (2013). A low-temperature solid-phase method to synthesize highly fluorescent carbon nitride dots with tunable emission. Chemical Communications. 49: 8605-7.
5. Fernandes, Diogo, Krysmann, Marta J, Kelarakis, et al (2015). Carbon dot based nanopowders and their application for fingerprint recovery. Chemical Communications. 51: 4902-4905.
6. Nicollian EH (1971). Surface Passivation of Semiconductors. Journal of Vacuum Science and Technology. 8 (5): S39-S49.
7. Mishra, Manish KR, Chakravarty, Amrita, Bhowmik, et al (2015). Carbon nanodot–ORMOSIL fluorescent paint and films. Journal of Materials Chemistry C. 3:714-9.
8. Zhou, Jigang (2013). An electrochemical approach to fabricating honeycomb assemblies from multiwall carbon nanotubes. Carbon. 59:130-139.
9. Mandal, Tapas K, Parvin, Nargish (2011). Rapid Detection of Bacteria by Carbon Quantum Dots. Journal of Biomedical Nanotechnology. 7:846-8.
10. Bhattacharya, Dipsikha, Mishra, Manish K, De, et al (2017). Carbon Dots from a Single Source Exhibiting Tunable Luminescent Colors through the Modification of Surface Functional Groups in ORMOSIL Films. Journal of Physical Chemistry C. 121: 28106-16.